DMD Fast Forward. Published on July 30, 2007 as doi:10.1124/dmd.107.016840

Title page

Serine hydroxymethyltransferase isoforms are differentially inhibited by leucovorin – *Characterization and comparison of recombinant zebrafish serine hydroxymethyltransferases*

Wen-Ni Chang, Jen-Ning Tsai, Bing-Hung Chen, Huei-Sheng Huang, Tzu-Fun Fu

Department of Medical Laboratory Science and Biotechnology, College of Medicine, National Cheng Kung University, Tainan 701, Taiwan (W.N.C, H.S.H, T.F.F); School of Medical Laboratory and Biotechnology, Chung Shan Medical University, Taichung, 402, Taiwan (J.N.T); Faculty of Biotechnology, Kaohsiung Medical University, Kaohsiung 807, Taiwan (B.H.C)

Running title page

Running Title: SHMTs differentially inhibited by leucovorin

Correspondence: Tzu-Fun Fu, Department of Medical Laboratory Science and Biotechnology, College of Medicine, National Cheng Kung University, No.1, University Road, Tainan 701, Taiwan. Tel.: 886-6-2353535 (ext. 5795); Fax: 886-6-236-3956; E-mail: tffu@mail.ncku.edu.tw.

The number of:

Text pages: 45

Tables: 2

Figures: 7

References: 40

Words in Abstract: 239

Words in Introduction: 750

Discussion: 1420

Abbreviations: SHMT, serine hydroxymethyltransferase; zmSHMT and zcSHMT refer to zebrafish mitochondrial and cytosolic SHMTs, respectively; hcSHMT and rcSHMT refer to the human cytosolic and rabbit cytosolic enzymes; THF, H_4PteGlu, tetrahydropteroylglutamate; N^5-CHO-H_4PteGlu, N^5-formyl-tetrahydropteroylglutamate; N^5,N^{10}-CH_2-, N^5,N^{10}-methylene; N^5-CH_3-, N^5-methyl; PLP, pyridoxal-5'-phosphate; MTX, methotrexate; TS, thymidylate synthase;

PCR, polymerase chain reaction; DHFR, dihydrofolate reductase; dTMP, deoxythymidine monophosphate; AdoMet, S-Adenosyl Methionine; hCys, homocysteine; EGFP, enhanced green fluorescent protein; IPTG, isopropyl-beta-D-thiogalactopyranoside; SDS-PAGE, sodium dodecyl sulfate polyacrylamide gel electrophoresis; NADPH, β-Nicotinamide adenine dinucleotide 2'-phosphate reduced tetrasodium.

DMD Fast Forward. Published on July 30, 2007 as DOI: 10.1124/dmd.107.016840
This article has not been copyedited and formatted. The final version may differ from this version.

Abstract

Serine hydroxymethyltransferase (SHMT) provides activated one-carbon units required for the biosynthesis of nucleotides, protein and methyl group by converting serine and tetrahydrofolate to glycine and N^5,N^{10}-methylenetetrahydrofolate. It is postulated that SHMT activity is associated with the development of methotrexate-resistance and the *in vivo* activity of SHMT is regulated by the binding of N^5-CHO-THF, the rescue agent in a high-dose methotrexate chemotherapy. The aim of this study is to advance our understanding in the folate-mediated one-carbon metabolism in zebrafish by characterizing zebrafish mitochondrial SHMT. The cDNA encoding zebrafish mitochondrial SHMT was cloned, overexpressed in *E.coli* and purified with a three-step purification protocol. Similarities in structural, physical and kinetic properties were revealed between the recombinant zebrafish mitochondrial SHMT and its mammalian orthologs. Surprisingly, leucovorin significantly inhibits the aldol cleavage of serine catalyzed by zebrafish cytosolic SHMT but to a less extent the reaction catalyzed by the mitochondrial isozyme. This is the first report on zebrafish mitochondrial folate enzyme as well as the differential inhibition of leucovorin on these two SHMT isoforms. Western blot analysis revealed tissue-specific distribution with the highest enrichment present in liver for both cytosolic and mitochondrial SHMTs. Intracellular localization was confirmed by confocal microscopy for both mitochondrial and cytosolic SHMTs. Unexpectedly, the cytosolic isoform was observed in both nucleus and cytosol. Together with the previous report

on zebrafish cytosolic SHMT, we suggest that zSHMTs can be used in *in vitro* assays for folate-related investigation and antifolate drug discovery.

Folates carry the chemically activated single carbons at N^5 and/or N^{10} positions and are required for the biosynthesis and metabolism of nucleic acid, protein, amino acid, methyl group, neurotransmitter, and vitamins. Its vital role in nucleotides biogenesis has led to development of many anticancer drugs targeting folate-requiring enzymes. Among them, methotrexate (MTX) is one of the most widely used anticancer agents to date. It blocks *de novo* nucleotide synthesis by depleting reduced tetrahydrofolates mainly through inhibition of dihydrofolate reductase (DHFR) and thymidylate synthase (TS) (Fig. 1, enzymes #2 and 3, respectively). However, resistance to MTX often emerges and becomes the major impediment to its curative potential. To overcome this obstacle and prevent MTX-associated toxicity, high-dose MTX combined with leucovorin rescue is administrated and has become an important regimen in the treatment for a variety of cancers (Frei, III, et al., 1980). Despite these preventive measures, MTX-induced resistance and toxicity continue to occur, though infrequently. Mechanisms including elevated DHFR, decreased TS, impaired folates/antifolates transportation and decreased polyglutamylation on MTX have been proposed to contribute to the development of MTX-resistance (Asai, et al., 2003). It is also postulated that the excessive use of leucovorin makes tumor cells refractory to subsequent MTX therapy (Bleyer, 1977;Sirotnak, et al., 1978). Nevertheless, what causes the emergence of MTX-resistant tumor cells and the reason why high concentrations of leucovorin might affect cells survival or even endorse MTX-resistance remain to be answered.

DMD Fast Forward. Published on July 30, 2007 as DOI: 10.1124/dmd.107.016840
This article has not been copyedited and formatted. The final version may differ from this version.

In vivo, N^5-CHO-THF, also known as leucovorin, is generated by the irreversible hydrolysis of N^5,N^{10}-CH^+-THF in a second reaction catalyzed by serine hydroxymethyltransferase (SHMT). N^5-CHO-THF also acts as a tight-binding inhibitor of the cytosolic form of SHMT (Stover and Schirch, 1991). SHMT is a pyridoxal-5'-phosphate (PLP) -dependent enzyme and reversibly converts serine and THF to glycine and N^5,N^{10}-CH_2-THF, the principal pathway of one-carbon unit incorporation in cells. One-carbon metabolism is compartmentalized with folate coenzymes equally distributed in cytosol and mitochondria (Appling, 1991). In higher organisms more than one SHMT isoform is often present: a cytosolic isoform and an organelle-associated form, usually mitochondria. Although the physiological functions of these two isozymes remain unclear, it is suggested that cytosolic SHMT (cSHMT) tends to function in the direction of serine synthesis, whereas the production of glycine and N^5,N^{10}-CH_2-THF is mainly catalyzed by mitochondrial SHMT (mSHMT) (Narkewicz, et al., 1996). Studies suggested that the activity of cSHMT is associated with the development of MTX resistance. It is believed that the cSHMT activity *in vivo* is modulated by the binding of N^5-CHO-THF and functions as a metabolic switch that shuttles the one-carbon unit between dTMP biosynthesis and homocysteine remethylation (Herbig, et al., 2002). Yet the effect of N^5-CHO-THF on mSHMT activity and the importance of mSHMT in leucovorin metabolism and MTX-resistance remain undetermined even though the uptake of N^5-CHO-THF by mitochondria has been shown to be rapid and concentration-dependent

(Horne, et al., 1992). Currently, the animal model employed for folate-related studies is restricted mostly to rodent for its resemblance with human in folate-requiring enzymes. However, deciphering the role of folate enzymes in early mammalian development might be limited due to the maternal contribution of folate coenzymes during embryogenesis (Marasas, et al., 2004). Considering the feature of external development, zebrafish might serve as a valuable alternative for folate-related studies since the maternal supply of folates and folate enzymes are likely to be depleted with time in developing embryos. Increasing studies also demonstrate comparable features between zebrafish and human in many biological pathways and pathogenesis, including organs development, angiogenesis, hemostasis, heart function and circulation, apoptosis and proliferation, carcinogenesis, drug abuse and addiction, and toxicology and teratogenicity (Kari, et al., 2007). However, folate-requiring one-carbon metabolism in zebrafish remains an unexplored territory, albeit its critical role in oncogenesis and fetal development in vertebrates.

Our previous study on the recombinant zebrafish cSHMT revealed strong similarities with mammalian orthologs, suggesting the appropriateness of using zebrafish as model for folate-related studies (Chang, et al., 2006). In the present report, we clone and characterize zebrafish mitochondrial SHMT (zmSHMT), the other isoform of SHMT which is less understood in mammals. To our knowledge, this is the first report on a mitochondrial folate enzyme from zebrafish that is successfully expressed and purified in *E. coli*. The

similarities revealed between zebrafish mSHMT and human orthologs add more confidence to the uses of zebrafish in folate-related studies and drug discovery. In addition, we observe differential inhibition mediated by MTX and leucovorin on the catalytic activity of these two isoforms. The potential contribution of this observation to the development of MTX-resistance is also discussed.

DMD Fast Forward. Published on July 30, 2007 as DOI: 10.1124/dmd.107.016840
This article has not been copyedited and formatted. The final version may differ from this version.

Materials and Methods

Materials. PCR primers were ordered from MDBio, Inc. (Taiwan). The SMART™ RACE amplification kit was purchased from Clontech, Inc. (California, US). Polymerase Chain Reaction (PCR) Master Mix was purchased from ABgene House (Surrey, UK). Restriction enzymes used for cloning procedures were purchased from either Invitrogen (Carlsbad, CA) or New England BioLabs, Inc (Maryland, US). The clone expressing rabbit N^5,N^{10}-methylenetetrahydrofolate dehydrogenase was a generous gift from Dr. Verne Schirch/Virginia Commonwealth University, Richmond, VA. US. The HPLC gel filtration column Alltech ProSphere SEC, 250 HR, S-200 (4.6 mm x 30.0 cm) was purchased from Alltech (Illinois, US). (6S)-Tetrahydrofolate monoglutamate and (6S) N^5-CHO-tetrahydrofolate monoglutamate were generous gifts from Dr. Moser (Merck Eprova AG), Switzerland. Mitotracker Red probes for confocal microscopy was purchased from Invitrogen (California, US). Polyvinylidene difluoride (PVDF) membranes were purchased from Millipore Corporation (MA, US). Both the Bradford assay reagent and BCA™ protein assay kit were purchased from Pierce (IL, US). Rabbit polyclonal anti-zcSHMT antibodies were produced by Genesis Biotech Inc., Taiwan, with the enzymes we provided. Goat anti-hmSHMT antibodies, horseradish peroxidase-conjugated goat anti-rabbit IgG and donkey anti-goat secondary antibody were purchased from Santa Cruz Biotechnology Inc. (California, US). The zebrafish liver epithelial cell line ZLE established by Miranda et al. was generously

provided by Dr. Jiann-Ruey Hong/NCKU, Taiwan. All other chemicals, including coenzymes, buffers, amino acids, and antibiotics were purchased from Sigma-Aldrich Chemical Co. (St. Louis, MO).

Fish care and preparation of cDNA library from zebrafish embryos. Zebrafish (*Danio rerio*, AB strain) were bred and maintained in a 14 h-10 h light-dark diurnal cycle according to the standard condition described by Westerfield (Westerfield, 2000). Embryos were staged according to Kimmel et al.(Kimmel, et al., 1995). Total RNA isolation and cDNA library construction from zebrafish embryos were performed with RNAzol B reagent (Tel-Test. Inc.) and the SMART-RACE cDNA Amplification Kit (Clonetech, Inc.) as described previously (Chang, et al., 2006).

Bacterial strains, plasmids and general cloning procedures. The *E. coli* strain XL1 Blue (*rec*A1, *end*A1, *gyr*A96, *thi-1*, *hsd*R17(r_K^-,m_K^+), *sup*E44, *rel*A1, *lac*$^-$) was used for the construction of clones. The *E. coli* strains HMS174(DE3) (F^- recA r_{k12}^- m_{k12}^+) and Rosseta (DE3) (F^- recA r_{k12}^- m_{k12}^+), which contain the T7 RNA polymerase gene, were used for protein expression. The pET43.1a plasmid and all the *E. coli* strains for cloning and expression were obtained from Novagen (Madison, WI). The materials and methods for the general cloning procedures were as previously described (Chang, et al., 2006).

Cloning of zmSHMT from zebrafish cDNA library by PCR-based cloning strategy. A PCR-based approach with degenerate primers was employed for the

DMD Fast Forward. Published on July 30, 2007 as DOI: 10.1124/dmd.107.016840
This article has not been copyedited and formatted. The final version may differ from this version.

amplification and cloning of SHMT-encoding sequences from a zebrafish cDNA mixture. Two degenerate primers (5'- TGGGGNGTNAAYGTNCA -3' and 5'- WDATRTGNGCCATRTC -3') corresponding to the conserved regions of SHMT amino acid sequences (WGVNVQ and DMAHIS) were designed for PCR with the following conditions: a denaturation of 94 ^{o}C for 5 min followed by 55 cycles of 94 ^{o}C for 30 s, 60 ^{o}C for 30 s and 72 ^{o}C for 90 s. The resultant products were cloned and sequenced. The deduced amino acid sequences of the amplified products fall into two categories and shared 70-90 % identity with the corresponding regions of SHMT. Genebank BLAST search revealed 100 % and 61% identity between these two sequences and zcSHMT cDNA (zebrafish *shmt1*, accession number: NM_201046). Based on the sequence information of the 61% identity fragment, we proceeded with the isolation of prospective zebrafish mitochondrial SHMT cDNA.

The cloning of full-length zmSHMT cDNA was accomplished by rapid amplification of cDNA ends (RACE) method using zmSHMT gene specific primers designed based on the sequence information of the cloned fragment (Scheme 1). The reverse primer SHMT II-1(R) (5'-AGCGATGATGAGTTTGGGTCTGAA-3') and the UPM primer provided in the SMART^{TM} RACE cDNA Amplification Kit (Clontech, CA) were used in the first round PCR reaction, with the 5'RACE cDNA mixture as template. The resultant bands were TA-cloned and sequenced. Based on the sequence information, two primers, SHMT II-2(F) (5'-AGAGTACGGGGGGGCTGTCATTTA -3') and SHMT II-3(F)

DMD Fast Forward. Published on July 30, 2007 as DOI: 10.1124/dmd.107.016840
This article has not been copyedited and formatted. The final version may differ from this version.

(5'-TGCTGACACTGACATTACGACAAA -3') were designed for subsequent PCR amplifications. The SMART 3'-RACE cDNA mixture was used as template in the second round PCR with primer pairs SHMT II-2(F) and UPM. The third round of PCR was conducted using the second round PCR product as template and the primer pairs SHMT II-3(F) and NUP provided in the kit. All of the above amplifications were performed by touchdown PCR. The cycling condition were 5 cycles of 94 ^{o}C for 30s and 72 ^{o}C for 3 min; 5 cycles of 94 ^{o}C for 30s, 70 ^{o}C for 30s and 72 ^{o}C for 3 min; 40 cycles of 94 ^{o}C for 30s, 68 ^{o}C for 30s and 72 ^{o}C for 3 min. The resulting 2700-bp fragment was identified by restriction mapping and sequencing. The assembling of 5'RACE and 3'RACE sequences revealed the prospective full-length zmSHMT cDNA. The final amplification of the complete 1.5 kb encoding sequence was accomplished by PCR with the 5'RACE cDNA library prepared from 3 day-post-fertilization embryos as template and the primer pair SHMT II-4(F),

5'-CCGGATCCATATGCTGACACTGACATTACG-3' (forward) and SHMT II-4(R),

5'-CCCTGATGAATTCGTTTAATGGTCGTGGAATCC-3' (reverse). To simplify the cloning procedure, two restriction enzyme sites: Nde I and EcoR I (underlined), were introduced into the primers. The PCR amplified product was cloned into the expression vector pET43.1a. Successful cloning was confirmed by both restriction enzyme digestion and DNA sequencing.

Removal of signal peptide and introduction of the first methionine residue was

DMD Fast Forward. Published on July 30, 2007 as DOI: 10.1124/dmd.107.016840
This article has not been copyedited and formatted. The final version may differ from this version.

accomplished by PCR using zmSHMT coding sequence as template with the primer pair: 5'-GCGCTCCTCCCATATGGTGTGTGTGCGC-3' (forward) and SHMT II-4(R) followed by cloning into the pET43.1a vector, yielding the clone zmSHMT(DelSig). The resultant constructs were transformed into an *E. coli* host cell Rosetta (DE3) for enzyme expression and purification.

Zebrafish SHMT-EGFP fusion plasmids were constructed by PCR cloning with the zcSHMT or zmSHMT plasmids and the primers designed to abolish stop codons and introduce BglII, EcoRI or SalI restriction enzyme sites. The primers were: 5'-GCGTTGGGAGATCTCCCATATG -3' (forward) and 5'- CAAGCAGAAAT GAATTCGTAACTCTGGCAACC -3' (reverse) for zcSHMT/pEGFP-N1; 5'-GCGTTGGGAG ATCTCCCATATG -3' (forward) and 5'-CCGCGGGAATTCGTCGACTGGTCGTGGAATCC -3' (reverse) for zmSHMT/pEGFP-N1.

Expression and purification of recombinant zmSHMT. All buffers described below for the purification of zSHMTs and kinetic studies contained 5 mM 2-mercaptoethanol, 0.2 mM EDTA and 2 μM PLP unless otherwise stated. Similar purification procedures for zcSHMT was applied to the purification of zmSHMT(DelSig) with minor modifications indicated below (Chang, et al., 2006). In brief, *E. coli* containing the desired plasmid was grown to log phase and enzyme induced at 25^{o}C with 0.08 mM IPTG for 3 hrs. Cells were harvested and lysed with lysozyme and chromatin removed by protamine sulfate precipitation.

DMD Fast Forward. Published on July 30, 2007 as DOI: 10.1124/dmd.107.016840
This article has not been copyedited and formatted. The final version may differ from this version.

After a 30% to 50% ammonium sulfate fractionation and desalted on a P-6DG column, zmSHMT(DelSig) was loaded onto a CM-Sephadex column (2.5 x 5.0 cm) and eluted with the linear salt gradient of 50 ml of equilibrating buffer and 50 ml of 500 mM potassium phosphate, pH 7.25. The purified enzyme was stored at -20^{o}C or -80^{o}C in the presence of 10 % glycerol. Protein from each step of the purification was examined by SDS-PAGE for purity.

Determination of physical properties. Apo-SHMTs were prepared by the removal of thiazolidine formed between L-Cys and active site PLP. Same principle was employed to determine the stoichiometry of PLP bound per molecule of enzyme with extinction coefficient of 5580 $M^{-1}cm^{-1}$for thiazolidine (Ulevitch and Kallen, 1977). The quaternary structure is determined on a Superdex 200 size-exclusion column as previously described (Chang, et al., 2006). The molar absorptivity coefficient was determined as stated by Gill and von Hippile previously (Gill and von Hippel, 1989).

Enzyme assays and inhibition. The rate of N^5,N^{10}-CH_2-THF formation catalyzed by SHMT can be continuously monitored at 340 nm by coupling with excess N^5,N^{10}-CH_2-THF dehydrogenase, which converts $NADP^+$ to NADPH. All kinetic constants were determined in 20 mM potassium phosphate buffer, pH 7.0 containing 0.4 mM $NADP^+$, 5 mM 2-mercaptoethanol and 0.5 μM methylenetetrahydrfolate dehydrogenase at 30 ^{o}C in a 1-cm cuvette. These studies include determination of k_{cat} and K_m values for substrates and inhibition by MTX and N^5-CHO-THF. L-Serine concentrations used in k_{cat} and K_m determination varied

DMD Fast Forward. Published on July 30, 2007 as DOI: 10.1124/dmd.107.016840
This article has not been copyedited and formatted. The final version may differ from this version.

from 0.07 to 0.75 mM in the presence of 0.15 mM THF. Reactions were initiated by adding 10 µg SHMT. Inhibition of initial velocity was determined in a 1-ml cuvette containing 20 mM phosphate, pH 7.3, 0.1 µM SHMT, 25 µM THF, 10 mM or 50 µM L-serine, saturated $NADP^+$ and inhibitors ranging from 0.1 to 100 µM for both N^5-CHO-THF and methotrexate.

Determination of dissociation constant for reduced folates. The dissociation constants for THF and N^5-CHO-THF of zmSHMT(DelSig) were measured by the formation of quinonoid complex in the presence of saturated glycine and reduced folates ranging from 2.5 to 54 µM (Chang, et al., 2006;Strong, et al., 1989). Results were analyzed with Scatchard plots and double-reciprocal plots, yielding K_d and stoichiometry of bound folates.

Fish tissue homogenization. Tissues or organs, including brain, eye, heart, liver, gastrointestinal tract and muscle, were obtained from adult zebrafish after the animals were euthanized by waterborne exposure to tricaine (ethyl 3-aminobenzoate, methanesulfonic acid, Sigma). Tissues were rapidly isolated, stored in 50 to 200 µl of phosphate buffered saline, pH 7.2 and kept on ice during the whole process of extraction. Homogenization was carried out in the phosphate-buffered saline lysis buffer containing a protease inhibitor cocktail consisting of AEBSF, Aprotinin, Leupeptin, Bestatin, Pepstatin A and E-64 (Sigma, Product No. P8340) and RNase inhibitor (Recombinant RNasin®, Promega). Homogenized samples were centrifuged at 10000 xg at 4 ^oC for 10 mins to remove particulate matter. Aliquots of the supernatant, about 10 to 30 µl, were subjected to Western blot and RT-PCR.

Western blot analysis. Supernatant protein content was determined using Bradford and BCA methods. Proteins of 20 μg were separated on a 10% SDS-separating gel and transferred to a polyvinylidene difloride membrane (PVDF) (Millipore). After blocking in blocking solution containing 5% non-fat milk, 0.1% Tween-20 in PBS overnight, the membrane was probed with anti-zcSHMT or anti-hmSHMT primary antibodies (1:1000 to 1:5000) and then horse-radish peroxidase-conjugated secondary antibody (1:5000). The PVDF membranes were also probed with anti-actin antibody for a loading control. The membrane was visualized using the SuperSignal™ chemiluminescent horseradish peroxidase substrate system from Pierce on FUJIFILM LAS-3000 imaging system. In the case of the gastrointestinal tract, where the signal for actin was not detectable, Ponceau-S staining was employed to verify equal loading.

We used the antibody against human mSHMT instead of zebrafish mSHMT to determine zmSHMT tissue distribution, owing to the concern of possible cross-reaction between zmSHMT and zcSHMT. The human mSHMT peptide sequence is 59 % and 76 % identical to zcSHMT and zmSHMT, respectively. The identity between zcSHMT and zmSHMT is 61%. We were hoping that the hmSHMT antibody will clearly distinguish zmSHMT from zcSHMT. As expected, no cross-reaction was detected even when we tested with 1 μg of purified proteins, allowing the uses of the antibodies as described.

RT-PCR analysis. For RT-PCR determination of SHMTs expression, total

mRNA was isolated from tissues using a Trizol kit (Invitrogen, Carlsbad, CA) following the manufacturer's instructions. After isolation, 1 μg of total mRNA in each tissue sample was reverse-transcribed with a high-capacity cDNA archive kit (Promega, Madison, WI), and 1 μl of the newly synthesized first strand cDNA library was used as template in the subsequent PCR analysis. The primer sequences are as follows: 5'- GGAGAGTCTGATTAATCAGGC -3'(F) and 5'- CATTTTGAGCCAGTTCCTCC -3'(R) for zcSHMT (505-bp fragment), 5'- GGAGAAGGTCAACTTC -3'(F) and 5'- GCGATTCGAGA AACCG -3'(R) for zmSHMT (523-bp fragment), and 5'- AGACATCAAGGAGAAGCTGTG -3'(F) and 5'- TCCAGACGGAGTATTTAC -3'(R) for β-actin (391-bp fragment) as a control for the RNA isolation and reverse-transcription. The annealing temperatures were 65^{o}C for zcSHMT, 60 ^{o}C for zmSHMT and 62 ^{o}C for β-actin . The PCR reaction condition was: 30 cycles of 30s at 94 ^{o}C, 30s at annealing temperature and 68 ^{o}C for 30s.

Determination of intracellular localization. ZLE cells were cultivated and regularly maintained in Leibovitz's L-15 medium supplemented with 5% fetal bovine serum at 28 ^{o}C. For transient transfection, ZLE cells of 1 x 10^{5}/ml were subcultured into 6-well plates 24 hours prior to transfection with zSHMTs/pEGFP-N1 fusion plasmids with a si-PORT transfection kit (Ambion). Cells were incubated for another 24 hours and co-stained with mitochondrial probe MitoTrackerDeep Red633 (Invitrogen) right before examining under a confocal microscope. Confocal microscopy images were acquired on a Leica TCS SP2

microscope.

DMD Fast Forward. Published on July 30, 2007 as DOI: 10.1124/dmd.107.016840
This article has not been copyedited and formatted. The final version may differ from this version.

Results

Cloning and sequence analysis of recombinant zmSHMT. The sequences of the 370 bps fragments resulted from PCR amplification with degenerate primers fall into two categories, designated as form-I and form -II. We had previously reported the cloning and characterization of zSHMT form-I, the prospective zcSHMT, which highly resembles mammalian cytosolic SHMT structurally and functionally (Chang, et al., 2006). The full length zSHMT-form II cDNA isolated is 1479 bp, which encodes a protein of 492 amino acids. Peptide sequence alignment with the known SHMT from other species and the prospective zcSHMT revealed a potential mitochondrial signal peptide cleavage site between residues 20 and 30. Signal peptide prediction using the software SignalP 3.0 (http://www.cbs.dtu.dk/services/) has narrowed the cleavage site down to Ala22 and Val24 and is in agreement to the reports for rabbit and human mitochondrial SHMTs (Fig. 2) (Martini, et al., 1989;Stover, et al., 1997). This prospective mitochondrial leader sequence of zSHMT-form II (we now designated as zmSHMT) is rich in arginine, leucine, threonine and serine and fulfills the criteria for a mitochondrial targeting sequence that locates at the N terminus of the precursor protein and contains 17 to 35 amino acids rich in positive charge. Both the conserved octapeptide encompassing a stretch of threonine residues and the lysine residue forming the internal aldimine with PLP are also identified in zmSHMT, further supporting the notion that zebrafish SHMTs are the orthologs of mammalian SHMTs (Fig. 2). The peptide sequence of

zmSHMT is 76% identical to its human ortholog, indicating a high conservation throughout evolution.

Expression and purification of zSHMTs. The overexpressed full-length zmSHMT with leader peptide resulted in the formation of insoluble precipitate in *E.coli* at all growth conditions we had tested, including lower temperatures, reduced inducer concentrations and addition of cofactor PLP and low molecular weight glycols (data not shown). The attempt to obtain a soluble and fully functional protein succeeded only after we performed a second PCR-based cloning to eliminate the predicted leader peptide that includes the first 23 amino acids. Induction for zmSHMT without signal peptide, designated as zmSHMT(DelSig), reaches an acceptable level with minimal production of insoluble enzyme (Fig. 3). Higher concentrations of IPTG, elevated induction temperature and/or prolonged induction time were found to increase the ratio of insoluble to soluble zmSHMT(DelSig), although the overall amount of induced enzyme is increased.

Similar purification protocol for zcSHMT and human SHMTs was applied to the purification for zmSHMT(DelSig) (Chang, et al., 2006;Kruschwitz, et al., 1995). After a 30 to 50% ammonium sulfate precipitation, the enzyme was 70% pure judged from SDS-PAGE with a two-fold purification (Table 1). We used gel filtration, instead of equilibrium dialysis, to remove ammonium sulfate since zmSHMT(DelSig) was found to precipitate after overnight dialysis. The zmSHMT(DelSig) bound to CM-Sephadex and was eluted at high salt.

Chromatographying on CM-Sephadex separates the endogenous enzyme from our cloned zmSHMT since most *E. coli* proteins, including *E.coli* SHMT, do not bind to cation exchange resins under these conditions (di Salvo, et al., 1998). Therefore, this step greatly simplifies the purification procedure and permits removing the great bulk of unwanted protein with a large fold of purification achieved. The SHMT eluted from this column was better than 98% pure (Fig. 3). From 2 liters of cells approximately 43 mg of pure zmSHMT(DelSig) was obtained with an overall yield of 90% (Table 1). The purified recombinant enzyme can be stored at -20 ^{o}C or -80 ^{o}C in the presence of 10% glycerol for at least six months without significant change in catalytic activity. However, frequent freeze-thaw cycles result in protein precipitation and loss of enzymatic activity.

Physical properties of zmSHMT(DelSig). The spectral properties of the recombinant zmSHMT(DelSig) appear to be similar to most of the studied SHMTs, including human (Chang, et al., 2006;di Salvo, et al., 1998;Kruschwitz, et al., 1995). Beside 278 nm, zmSHMT (DelSig) displays a distinct absorbance peak at 428 nm corresponding to the internal aldimine formed between PLP and an active site lysine residue (Fig. 4). The 428-nm peak in all other studied SHMTs gives a distinct spectral change in the presence of glycine and reduced folates due to the formation of a quinonoid ternary complex absorbing near 500 nm. This long wavelength absorbance is attributed to a glycine anion in resonance with the bound pyridoxal phosphate and has been used extensively to determine the binding constants of

tetrahydrofolates and glycine (Schirch, 1982). The same properties were observed for the recombinant zmSHMT(DelSig) (Fig. 4).

The predicted molar absorptivity coefficient at 278 nm for denatured zmSHMT(DelSig) was 39,910 $M^{-1}cm^{-1}$, based on amino acid composition. The coefficient of the native enzyme was obtained by multiplying the predicted value by the ratio of absorbance at 278 nm of denatured and native states, yielding a molar absorptivity coefficient of zmSHMT(DelSig) ε_{278} = 45,893 $M^{-1}cm^{-1}$. This shows that a 1 mg/ml solution of zmSHMT(DelSig) holoenzyme will exhibit absorption of 0.88 at 278 nm. This is slightly higher, but comparable to zcSHMT, which has a molar absorptivity coefficient of 45,060 $M^{-1}cm^{-1}$ (Chang, et al., 2006). The Trp residues contained in zcSHMT and zmSHMT are two and three, respectively.

SDS-PAGE showed a single band of approximately 50 kDa for the recombinant zmSHMT(DelSig) (Fig. 3). This compares to the calculated size of 51,912 Da based on the peptide sequence of a zmSHMT(DelSig) monomer. Both holo- and apo-zmSHMT (DelSig) had a Stokes radius close to a globular protein of 200 kDa and were eluted at the same retention volume as zcSHMT and human cytosolic SHMT tetramers on a Superdex 200 column (data not shown). These results suggest a homotetrameric structure for the recombinant zmSHMT(DelSig).

L-cysteine forms a thiazolidine compound with the active site PLP which can be

removed by dialysis or precipitation of the protein, providing a simple method for preparing mitochondrial apo-SHMT and determination of PLP binding stoichiometry (Ulevitch and Kallen, 1977). Our results show that one PLP molecule binds to each zmSHMT(DelSig) monomer, as observed for zcSHMT and most of the SHMTs studied to date (data not shown).

Steady-state kinetic constants and reduced folate affinity. Double-reciprocal plots of initial velocity versus serine concentration permits the determination of both apparent K_m for serine and k_{cat}. As shown in Table 2, both the K_m for serine and k_{cat} of zmSHMT(DelSig) are comparable to the values for zcSHMT and rabbit mitochondrial SHMT. The enzyme remains fully active at 37 ^{o}C for at least 30 mins (data not shown).

The quinonoid intermediate formed between reduced folates and the active site PLP absorbs near 500 nm with a molar extinction coefficient of 40,000 $M^{-1}cm^{-1}$ (Schirch, et al., 1977). This absorbance shows saturation kinetics with most reduced folate substrates including $H_4PteGlu_n$, N^5-CHO-$H_4PteGlu_n$ and N^5-CH_3-$H_4PteGlu_n$ (Schirch and Ropp, 1967;Stover and Schirch, 1991). The binding of substrates to rabbit cytosolic SHMT is a sequential random mechanism. Previous studies had confirmed that the K_d determined by this method were essentially the same as K_m for folate determined from kinetic measurements (Schirch, et al., 1977;Szebenyi, et al., 2004). However, the reported value is an apparent K_d because the formation of this complexes is at least a two-step process. The lower K_d of zmSHMT(DelSig) for THF suggests a higher affinity for this substrate when compared to zcSHMT. Both

isoforms have comparable affinity for N^5-CHO-THF, judged from their similar dissociation constants (Table 2).

Inhibition of SHMT aldol cleavage activity. Increasing concentrations of leucovorin (N^5-CHO-THF) inhibit both zcSHMT and hcSHMT activities substantially, yet to a less extent to zmSHMT (Fig. 5). The inhibitions of SHMT catalyzed serine aldol cleavage by leucovorin and MTX were determined for zc-, zm- and hcSHMT. Approximately 70 % and 30% inhibition were observed for zc- and zmSHMT(DelSig) activities, respectively, in the presence of 70 μM of N^5-CHO-THF (Fig. 5A). The IC_{50} of leucovorin is approximately 30 μM for zcSHMT and higher than 70 μM for zmSHMT. The differential inhibition is evident with the presence of 10 μM leucovorin, the concentration estimated in serum in a high-dose leucovorin rescue regimen. Similar pattern of inhibition but even larger difference between zc- and zmSHMT was observed when the inhibition was assayed in the presence of 50 μM serine (Fig. 5B). MTX also represses SHMTs activities, but not as significantly as to zDHFR activity (Fig. 5C and TF Fu, unpublished result). No significant difference was observed when the highest concentrations of leucovorin (70 μM) and MTX (100 μM) were added simultaneously to the reaction in a combined assay as compared to adding leucovorin alone (data not shown).

Tissue specific distribution of zmSHMT and zcSHMT isoforms. RT-PCR results showed that zmSHMT mRNA was evenly distributed among tissues, whereas significantly

higher levels of zcSHMT mRNA were detected in heart, liver, and ova (Fig. 6C). This result is in agreement with the ubiquitous distribution of human mSHMT message and tissue-specific expression of cSHMT mRNA (Girgis, et al., 1998). PCR was also performed using plasmids containing zcSHMT or zmSHMT coding sequences as templates to validate the positive signal. No PCR product was observed in this cross-reaction test (Fig. 6A).

Interestingly, we found that the SHMT proteins levels did not correspond to their mRNA amounts detected in most of the tissues examined. Strong tissue-specificity was observed in protein levels for both zcSHMT and zmSHMT (Fig. 6C). Zebrafish cSHMT protein was predominant in liver and also abundant in ova. Significant zmSHMT protein was detected only in liver and gastrointestinal tract regardless of the evenly distributed mRNA message. We also noted that appreciable amounts of cSHMT, but not mSHMT, were found in unfertilized eggs in both mRNA and protein levels. Equal loading of samples was confirmed by the presence of β –actin, Ponceau-S staining of the membrane and Coomassie Brilliant Blue stained SDS-polyacrylamide gel.

Subcellular localization of zebrafish SHMTs. The prediction on the recombinant zSHMTs intracellular localization was confirmed by the site-specific compartmentalization of EGFP-fused SHMTs with confocal microscopy. The overexpressed zmSHMT-EGFP was clearly co-localized with a mitochondrial marker, demonstrating the mitochondrial localization of this enzyme (Fig. 7A). For zcSHMT-EGFP, surprisingly, the

fluorescence signal of various intensities was detected in both nucleus and cytosol. No signal corresponding to free GFP was detected in cell extracts prepared from zcSHMT-EGFP transformants, excluding the possibility of artifacts or false signal due to any undesired sample contamination (Fig. 7B).

DMD Fast Forward. Published on July 30, 2007 as DOI: 10.1124/dmd.107.016840
This article has not been copyedited and formatted. The final version may differ from this version.

Discussion

Despite the unknown biological function and significance of SHMTs, studies showed that impairment of SHMT activity resulted in disturbance of homeostasis of intracellular one-carbon pool and led to pathogeneses including homocysteinemia, cancers, cardiovascular diseases and neural tube defects, implying a crucial role of SHMT in normal cell growth and functions (Stover and Garza, 2006). The existence of both cytosolic and mitochondrial SHMTs has been known since Nakano et al. partially purified the enzyme from rat liver mitochondria in 1968 (Nakano, et al., 1968). Since then, cytosolic SHMT of many species have been studied thoroughly; whereas, the information about mitochondrial isoform is still very limited.

We report here the cloning and characterization of zebrafish mitochondrial SHMT. The identity of this recombinant protein was confirmed by its serine aldol cleavage activity and co-localization with MitoTraker Red®, a mitochondrial specific dye. The full length zmSHMT expressed in *E. coli* forms inclusion body. This result was not unexpected since expression of organelles specific proteins containing signal peptide often leads to formation of insoluble protein. Further characterization of zmSHMT(DelSig) reveals substantial similarities in its structure, physical properties and kinetics to zcSHMT and mammalian orthologs, adding confidence to using zebrafish as an animal model for folate-related studies. That similar protocols applied to the purification of hcSHMT, rcSHMT, zcSHMT and

DMD Fast Forward. Published on July 30, 2007 as DOI: 10.1124/dmd.107.016840
This article has not been copyedited and formatted. The final version may differ from this version.

zmSHMT(DelSig) suggests comparable surface properties among these isoforms. Surprisingly, no evident cross-reaction between anti-zcSHMT antibody and zmSHMT(DelSig) protein was detected in Western blot analysis, despite a 63% identity was found in their peptide sequences. The possible explanation is that the homologous sequences might be embedded inside and therefore were not exposed to lymphocytes recognition and antibody generation.

It is interesting to notice that the aldol cleavage of serine catalyzed by zc- and zmSHMTs were differentially inhibited by N^5-CHO-THF (leucovorin), despite both enzymes bind to this compound with similar affinity. To our knowledge, this is the first report on the effect of leucovorin on mitochondrial SHMT. The concentrations of serine and THF used in the inhibition assays encompassing the physiological concentrations of both substrates, implying that the similar inhibition pattern might also occur *in vivo* (Vinnars, et al., 1975). The differential inhibition observed between these two isoforms might be attributed to the lower K_d of zmSHMT than zcSHMT for THF. Stover and colleagues suggested that N^5-CHO-THF binds and modulates cSHMT activity, enabling this enzyme to function as a regulatory switch in one-carbon metabolism. When activated, the cSHMT-derived N^5,N^{10}-CH_2-THF gives thymidylate synthetic pathway higher metabolic priority than homocysteine remethylation cycle (Herbig, et al., 2002;Woeller, et al., 2007). The later one generates S-adenosylmethionine (AdoMet), the major methyl donor for most intracellular methylation including DNA and protein. Our results add further weight to the notion that zmSHMT is responsible for a stable

supply of N^5,N^{10}-CH_2-THF; whereas cSHMT is sensitive to alteration in nutritional status and functions to regulate the one-carbon flow in a changed environment (Stover and Garza, 2006). In a high-dose MTX combined leucovorin rescue therapy the differential inhibitory effects of N^5-CHO-THF to zc- and zmSHMT might result in decreased ratio of THF/ N^5,N^{10}-CH_2-THF hence re-distribution of the activated one-carbon units between nucleotide biosynthesis and cellular methylation, yielding profound impact in intracellular events, gene activities and ultimately, cell survival. Evidences supporting that cSHMT activity might play a role in the development of MTX-resistance have been reported. In support of this notion are that polymorphism in cSHMT was related to MTX-resistance in pediatric patients with acute lymphoblastic leukemia and overexpression of cSHMT in *Leishmania* increased resistance to methotrexate in a rich folate containing medium (de Jonge, et al., 2005;Gagnon, et al., 2006). The present study adds mSHMT to the picture for possible mechanistic insights and provides clues to further understand the complex relationships between one-carbon metabolism, SHMTs, and the development of MTX-resistance.

The MTX and leucovorin concentrations used in the inhibition studies ranged from 0.1 to 100 μM. It was estimated that a concentration of 1-10 μM for both MTX and leucovorin is a realistic serum concentration that can be reached in MTX-leucovorin combined regimen (Widemann and Adamson, 2006). However, we are convinced that the differential inhibition observed in our studies should have reflected what have occurred *in vivo* since the

DMD Fast Forward. Published on July 30, 2007 as DOI: 10.1124/dmd.107.016840
This article has not been copyedited and formatted. The final version may differ from this version.

polyglutamylation of folates/antifolates substrates will significantly increase their affinities to folate enzymes. Five to seven glutamate residues will be added to the γ-carboxyl group of the internalized MTX and N^5-CHO-THF. Studies showed that the K_d to rabbit cSHMT were closed to 5 μM for both $H_4PteGlu_1$ and N^5-CHO-$H_4PteGlu_1$; whereas the K_d to the same enzyme are 0.056 and 0.02 mM for $H_4PteGlu_5$ and N^5-CHO-$H_4PteGlu_5$, respectively (Fu, et al., 2005;Huang, et al., 1998). It implies that the inhibition mediated by N^5-CHO-$H_4PteGlu_5$ in cells should be comparable to, if not more significant than, the results observed in *in vitro* studies since polyglutamylation will further potentiate the competitivity of polyglutamylated-leucovorin with tetrahydrofolatepolyglutamate.

Tissue-specific expression was evident in protein level for both SHMT isozymes in zebrafish with the highest expression in liver. This is the first report on the tissue specific distribution of mitochondrial SHMT. It was documented that human mSHMT mRNA was evenly expressed among tissues (Girgis, et al., 1998). Interestingly, our RT-PCR results for zmSHMT was in agreement to human mSHMT expression pattern and showed equal distribution, suggesting that translational and/or post-translational regulation might play a role in controlling the intracellular concentrations of both enzymes. Protein stabilized by the binding of folate substrates and/or PLP cofactor might also contribute to the different protein levels observed in this study. Support to this notion is a very recent report showing that lack of vitamin B6 in cells causes decrease in SHMT protein but not mRNA level (Perry, et al.,

2007). Notably, cSHMT is abundant in unfertilized eggs, supporting the view that SHMT is a maternally essential gene (Vatcher, et al., 1998). Studies on the correlation between the abundance of SHMTs and potential risk of developing MTX-resistance might be rewarded in understanding the differential efficacy of MTX observed in various types of cancer.

We were first puzzled and vigilant when we observed the presence of zcSHMT in nucleus, since the nuclear localization of cSHMT has never been reported by then. Negative result was obtained when the peptide sequence was subjected to search for specific nuclear-targeting sequence. Having repeated this experiment carefully and revealed the same results many times prompted us to postulate that the zcSHMT-EGFP might be transported into nucleus via cargo or other components-mediated mechanism. Interestingly, our observation and hypothesis was found later to be in agreement to what was reported by Woeller et al. in a very recent study that human cSHMT was SUMOylated and nuclear-localized in a cell-cycle dependent manner (Woeller, et al., 2007). Two prospective SUMOylation sites are identified in zcSHMT peptide sequence, suggesting a possible similar mechanism for zcSHMT nuclear localization and resemblance between human and zebrafish SHMTs. The biological significance of the nuclear-localized cSHMT is unknown. Yang and colleagues showed that cSHMT was in some way connected to the nucleolar protein SRP40p and modulated cell cycle and cell size, supporting a non-catalytic function of cSHMT (Yang and Meier, 2003). Enlargement of the cell size was also observed in our zcSHMT-EGFP transfected cells. The

significance of zcSHMT intracellular localization is currently under investigation.

Zebrafish has attracted many researchers' interests as an animal model in the past two decades. The features of external development, transparent embryo, ease of growth and breeding, economy and can easily be manipulated using well-established molecular approaches have made zebrafish an ideal animal model for studying developmental biology and pathogenic mechanisms in a variety of conditions. Especially important for drug discovery is that zebrafish embryos are permeable to small molecules and drugs during organogenesis, providing easy access for drug administration and vital dye staining (Kari, et al., 2007). It is undoubted that efforts will be continuously invested in the improvement of antifolate drugs, considering the vital role of folates in nucleotides and protein biosynthesis. The search for new targets of antifolate drugs will also be sustained. In addition to its vital role in folate-mediated one-carbon metabolism, the property of being highly expressed in rapidly proliferating cells has made SHMT a potential target for chemotherapy and immunosuppresion (Renwick, et al., 1998). Our studies conclude that zebrafish SHMTs share high similarity with human isozymes, indicating that zSHMTs, and probably zebrafish as a whole, are appropriate systems for folate-related studies and antifolate drugs discovery. Further studies on other folate enzymes should be warrant. In addition, the possible mechanistic insights provided in this study enable us to further understand the complex relationships between one-carbon metabolism, SHMTs, and the development of

MTX-resistance.

Acknowledgements

Our sincere appreciation goes to Dr. Verne Schirch/Virginia Commonwealth University for his valuable advice and assistance. We also thank Dr. Moser/ Merck Eprova AG and Dr. Jiann-Ruey Hong/National Cheng Kung University for the precious materials they generously provided.

References

Appling DR (1991) Compartmentation of folate-mediated one-carbon metabolism in eukaryotes. *FASEB J* **5**:2645-2651.

Asai S, Miyachi H, Kobayashi H, Takemura Y and Ando Y (2003) Large diversity in transport-mediated methotrexate resistance in human leukemia cell line CCRF-CEM established in a high concentration of leucovorin. *Cancer Sci* **94**:210-214.

Bleyer WA (1977) Methotrexate: clinical pharmacology, current status and therapeutic guidelines. *Cancer Treat Rev* **4**:87-101.

Chang WN, Tsai JN, Chen BH and Fu TF (2006) Cloning, expression, purification, and characterization of zebrafish cytosolic serine hydroxymethyltransferase. *Protein Expr Purif* **46**:212-220.

de Jonge R, Hooijberg JH, van Zelst BD, Jansen G, van Zantwijk CH, Kaspers GJ, Peters GJ, Ravindranath Y, Pieters R and Lindemans J (2005) Effect of polymorphisms in folate-related genes on in vitro methotrexate sensitivity in pediatric acute lymphoblastic leukemia. *Blood* **106**:717-720.

di Salvo ML, Delle FS, De BD, Bossa F and Schirch V (1998) Purification and characterization of recombinant rabbit cytosolic serine hydroxymethyltransferase. *Protein Expr Purif* **13**:177-183.

Frei E, III, Blum RH, Pitman SW, Kirkwood JM, Henderson IC, Skarin AT, Mayer RJ, Bast RC, Garnick MB, Parker LM and Canellos GP (1980) High dose methotrexate with leucovorin rescue. Rationale and spectrum of antitumor activity. *Am J Med* **68**:370-376.

Fu TF, Hunt S, Schirch V, Safo MK and Chen BH (2005) Properties of human and rabbit cytosolic serine hydroxymethyltransferase are changed by single nucleotide polymorphic mutations. *Arch Biochem Biophys* **442**:92-101.

Gagnon D, Foucher A, Girard I and Ouellette M (2006) Stage specific gene expression and cellular localization of two isoforms of the serine hydroxymethyltransferase in the protozoan parasite Leishmania. *Mol Biochem Parasitol* **150**:63-71.

Gill SC and von Hippel PH (1989) Calculation of protein extinction coefficients from amino acid sequence data. *Anal Biochem* **182**:319-326.

Girgis S, Nasrallah IM, Suh JR, Oppenheim E, Zanetti KA, Mastri MG and Stover PJ (1998)

Molecular cloning, characterization and alternative splicing of the human cytoplasmic serine hydroxymethyltransferase gene. *Gene* **210**:315-324.

Herbig K, Chiang EP, Lee LR, Hills J, Shane B and Stover PJ (2002) Cytoplasmic serine hydroxymethyltransferase mediates competition between folate-dependent deoxyribonucleotide and S-adenosylmethionine biosyntheses. *J Biol Chem* **277**:38381-38389.

Horne DW, Holloway RS and Said HM (1992) Uptake of 5-formyltetrahydrofolate in isolated rat liver mitochondria is carrier-mediated. *J Nutr* **122**:2204-2209.

Huang T, Wang C, Maras B, Barra D and Schirch V (1998) Thermodynamic analysis of the binding of the polyglutamate chain of 5-formyltetrahydropteroylpolyglutamates to serine hydroxymethyltransferase. *Biochemistry* **37**:13536-13542.

Kari G, Rodeck U and Dicker AP (2007) Zebrafish: An Emerging Model System for Human Disease and Drug Discovery. *Clin Pharmacol Ther*.

Kimmel CB, Ballard WW, Kimmel SR, Ullmann B and Schilling TF (1995) Stages of embryonic development of the zebrafish. *Dev Dyn* **203**:253-310.

Kruschwitz H, Ren S, Di SM and Schirch V (1995) Expression, purification, and characterization of human cytosolic serine hydroxymethyltransferase. *Protein Expr Purif* **6**:411-416.

Marasas WF, Riley RT, Hendricks KA, Stevens VL, Sadler TW, Gelineau-van WJ, Missmer SA, Cabrera J, Torres O, Gelderblom WC, Allegood J, Martinez C, Maddox J, Miller JD, Starr L, Sullards MC, Roman AV, Voss KA, Wang E and Merrill AH, Jr. (2004) Fumonisins disrupt sphingolipid metabolism, folate transport, and neural tube development in embryo culture and in vivo: a potential risk factor for human neural tube defects among populations consuming fumonisin-contaminated maize. *J Nutr* **134**:711-716.

Martini F, Maras B, Tanci P, Angelaccio S, Pascarella S, Barra D, Bossa F and Schirch V (1989) The primary structure of rabbit liver mitochondrial serine hydroxymethyltransferase. *J Biol Chem* **264**:8509-8519.

Nakano Y, Fujioka M and Wada H (1968) Studies on serine hydroxymethylase isoenzymes from rat liver. *Biochim Biophys Acta* **159**:19-26.

Narkewicz MR, Sauls SD, Tjoa SS, Teng C and Fennessey PV (1996) Evidence for intracellular partitioning of serine and glycine metabolism in Chinese hamster ovary cells. *Biochem J* **313 (Pt 3)**:991-996.

Perry C, Yu S, Chen J, Matharu KS and Stover PJ (2007) Effect of vitamin B(6) availability on serine hydroxymethyltransferase in MCF-7 cells. *Arch Biochem Biophys*.

Renwick SB, Snell K and Baumann U (1998) The crystal structure of human cytosolic serine hydroxymethyltransferase: a target for cancer chemotherapy. *Structure* **6**:1105-1116.

Schirch L (1982) Serine hydroxymethyltransferase. *Adv Enzymol Relat Areas Mol Biol* **53**:83-112.

Schirch L and Peterson D (1980) Purification and properties of mitochondrial serine hydroxymethyltransferase. *J Biol Chem* **255**:7801-7806.

Schirch L and Ropp M (1967) Serine transhydroxymethylase. Affinity of tetrahydrofolate compounds for the enzyme and enzyme-glycine complex. *Biochemistry* **6**:253-257.

Schirch LV, Tatum CM, Jr. and Benkovic SJ (1977) Serine transhydroxymethylase: evidence for a sequential random mechanism. *Biochemistry* **16**:410-419.

Sirotnak FM, Moccio DM and Dorick DM (1978) Optimization of high-dose methotrexate with leucovorin rescue therapy in the L1210 leukemia and sarcoma 180 murine tumor models. *Cancer Res* **38**:345-353.

Stover P and Schirch V (1991) 5-Formyltetrahydrofolate polyglutamates are slow tight binding inhibitors of serine hydroxymethyltransferase. *J Biol Chem* **266**:1543-1550.

Stover PJ, Chen LH, Suh JR, Stover DM, Keyomarsi K and Shane B (1997) Molecular cloning, characterization, and regulation of the human mitochondrial serine hydroxymethyltransferase gene. *J Biol Chem* **272**:1842-1848.

Stover PJ and Garza C (2006) Nutrition and developmental biology--implications for public health. *Nutr Rev* **64**:S60-S71.

Strong WB, Cook R and Schirch V (1989) Interaction of tetrahydropteroylpolyglutamates with two enzymes from mitochondria. *Biochemistry* **28**:106-114.

Szebenyi DM, Musayev FN, di Salvo ML, Safo MK and Schirch V (2004) Serine hydroxymethyltransferase: role of glu75 and evidence that serine is cleaved by a retroaldol mechanism. *Biochemistry* **43**:6865-6876.

Ulevitch RJ and Kallen RG (1977) Purification and characterization of pyridoxal 5'-phosphate dependent serine hydroxymethylase from lamb liver and its action upon beta-phenylserines. *Biochemistry* **16**:5342-5350.

Vatcher GP, Thacker CM, Kaletta T, Schnabel H, Schnabel R and Baillie DL (1998) Serine hydroxymethyltransferase is maternally essential in Caenorhabditis elegans. *J Biol Chem* **273**:6066-6073.

Vinnars E, Bergstom J and Furst P (1975) Influence of the postoperative state on the intracellular free amino acids in human muscle tissue. *Ann Surg* **182**:665-671.

Westerfield M (2000) *The zebrafish book*. Eugene: University of Oregon Press.

Widemann BC and Adamson PC (2006) Understanding and managing methotrexate nephrotoxicity. *Oncologist* **11**:694-703.

Woeller CF, Anderson DD, Szebenyi DM and Stover PJ (2007) Evidence for SUMO-dependent nuclear import of the thymidylate biosynthesis pathway. *J Biol Chem*.

Yang Y and Meier UT (2003) Genetic interaction between a chaperone of small nucleolar ribonucleoprotein particles and cytosolic serine hydroxymethyltransferase. *J Biol Chem* **278**:23553-23560.

Footnotes

This work was supported by Grant NSC 95-2320-B-006-022 from the National Science Council, Taiwan.

Chang WN and Fu TF equally contributed to this work.

The GenBank accession numbers in figure 2 are: human cytosolic SHMT, (NP_004160); human mitochondrial SHMT, (NP_005403); rabbit cytosolic SHMT, (P07511); rabbit mitochondrial SHMT, (P14519); zebrafish cytosolic SHMT, (NP_957340) and zebrafish mitochondrial SHMT, (EF213101).

DMD Fast Forward. Published on July 30, 2007 as DOI: 10.1124/dmd.107.016840
This article has not been copyedited and formatted. The final version may differ from this version.

Legends for figures

Fig. 1. The folate-mediated one-carbon metabolism involving both cytosolic and mitochondrial serine hydroxymethyltransferases. Folate coenzymes are equally distributed in cytosolic and mitochondrial compartments. Three cycles are involved in this pathway and are responsible for thymidylate, purine and methionine biosynthesis. The enzymes participate in this pathway are serine hydroxymethyltransferase (1), dihydrofolate reductase (2), thymidylate synthase (3), glycinamide ribonucleotide transformylase and 5-amino-4-imidazolecarboxamide ribotide transformylase (4), N^5,N^{10}-methenyltetrahydrofolate cyclohydrolase (5), N^5,N^{10}-methylenetetrahydrofolate dehydrogenase (6), N^5,N^{10}-methylenetetrahydrofolate reductase (7), and methionine synthase (8). A parallel pathway also exists in mitochondria where the activated one-carbon unit is generated in the serine aldol cleavage catalyzed by mitochondrial serine hydroxymethyltransferase (1*).

Fig. 2. Alignment of SHMT peptide sequences. The shaded characters indicate the identical amino acids. Gaps, indicated by hyphens, are introduced for optimal alignment. The arrowhead indicates the conserved lysine residue that is in a highly conserved octapeptide threonine stretch and forms the internal aldimine with PLP. The arrow indicates the first residue in zmSHMT(DelSig). The sequences were aligned using the Clustal W method with MegAlign/DNAstar sequence analysis software. The identities shared between zmSHMT and human and rabbit mitochondrial SHMT

are 75.4% and 76.0%, respectively. The GenBank accession numbers of the aligned sequences are listed in **Footnote**.

Fig. 3. SDS-PAGE of zmSHMT(DelSig) at each step of purification. Lane 1, lysate of cells without induction; lane 2, lysate of cells induced with IPTG; lane 3, after ammonium sulfate precipitation; lane 4, after CM column; lane 5, overloaded purified zmSHMT(DelSig).

Fig. 4. Absorbance of zebrafish SHMTs and its complexes with glycine and folate substrates. (A) Spectrum of zcSHMT (solid line) and zmSHMT(DelSig)(dotted line) in 20 mM potassium phosphate at pH 7.0. (B) Spectrum of zmSHMT(DelSig) (curve 1), zmSHMT(DelSig) saturated with glycine (curve 2), zmSHMT(DelSig) saturated with glycine and H_4PteGlu (curve 3), and zmSHMT(DelSig) saturated with glycine and N^5-CHO-H_4PteGlu (curve 4).

Fig. 5. Inhibition of the SHMT catalyzed serine aldol cleavage by increasing concentrations of leucovorin (N^5-CHO-THF) (A, B) and methotrexate (C). Inhibition on initial velocity was determined at 30^{o}C in the presence of 25 μM H_4PteGlu, saturated $NADP^+$, 10 mM (A, C) or 50 μM (B) serine, 0.1μM SHMT and inhibitors ranging from 0.1 to 100 μM.

Fig. 6. Tissue distribution of zebrafish cytosolic and mitochondrial SHMTs. (A) Plasmids (20 ng)

containing SHMTs coding sequences were used as templates in PCR reactions for specificity determination with the primer pairs indicated. (B) Anti-zcSHMT and anti-hmSHMT antibodies were tested against purified zcSHMT and zmSHMT for specificity. One microgram of each purified protein was subjected to SDS-PAGE and analyzed by Coomassie Brilliant Blue staining (upper panel) and Western blotting with anti-hmSHMT (middle panel) and anti-zcSHMT (lower panel) antibodies. (C) Individual tissues were prepared for Western blot (upper panel) and RT-PCR (lower panel) analysis from adult female zebrafishes as described in *Materials and Methods*. (D) Tissue extracts containing 20 μg of protein were separated by 10% SDS-PAGE and visualized by Coomassie Brilliant Blue staining. Figures presented here are representative figures of six independent repeats.

Fig. 7. Localization of EGFP-Tagged zSHMTs in ZLE cells. (A) The EGFP fusion constructs with zmSHMT (top panel) or zcSHMT (middle and bottom panels) fused to the N-terminus of EGFP were transiently transfected into ZLE cells and live confocal images were taken at 24 hours after transfection. The scales at the lower-right hand corner for zmSHMT-EGFP and zcSHMT-EGFP transformants are 8.00 μm and 20.00 μm, respectively. (B) Extract containing 20μg of protein prepared from cells transfected with plasmid generating free EGFP (lane 1) or zcSHMT-EGFP fusion protein (lane 2) were subjected to 10% SDS-PAGE and Western blot analysis with antibodies indicated on the top.

DMD Fast Forward. Published on July 30, 2007 as DOI: 10.1124/dmd.107.016840
This article has not been copyedited and formatted. The final version may differ from this version.

TABLE 1

Summary of recombinant zmSHMT(DelSig) purification

Step	Volume (ml)	Protein (mg)	Total activity (U)	Specific activity (U/mg)	Yield (%)	Purification (fold)
Cell lysate	19	537	736	1.37	100	1
$(NH_4)_2SO_4$	15	297	825	2.77	120	2
CM	2	43	658	15.3	90	11.2

DMD Fast Forward. Published on July 30, 2007 as DOI: 10.1124/dmd.107.016840
This article has not been copyedited and formatted. The final version may differ from this version.

TABLE 2

Comparison of kinetic parameters for recombinant zmSHMT(DelSig) with zcSHMT and rmSHMT

Apparent K_m and V_{max} values were determined by fitting the data to the Michaelis-Menten equation using Sigma Plot.

Species	αK_m for serine (mM)	αK_d for H_4PteGlu (μM)	αK_d for N^5-CHO-H_4PteGlu (μM)	Turnover number (min^{-1})	References
Zebrafish m[a]	0.43	8	2.8	537	Present report
Zebrafish c[b]	0.22	18	2.6	351	Chang et al. (Chang, et al., 2006)
Rabbit m[c]	0.60	25	10	500	Schirch et al. (Schirch and Peterson, 1980)

[a] zebrafish mSHMT(DelSig); [b] cytosolic SHMT; [c] mitochondrial SHMT

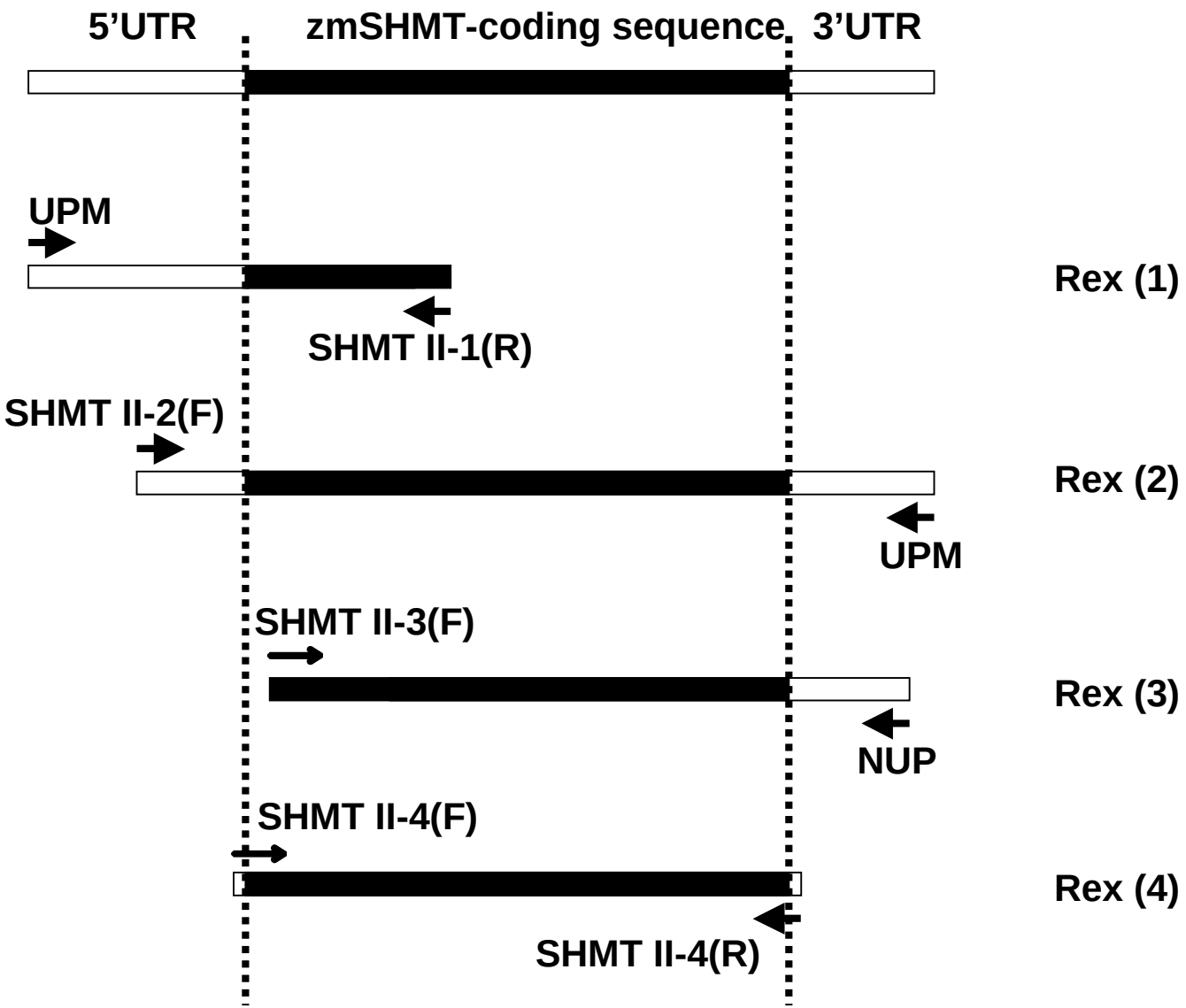

Scheme 1. PCR-based cloning of mitochondrial SHMT from the first-strand RACE-cDNA library prepared from 24-hr zebrafish embryos. UPM: Universal Primer Mix; NUP: Nested Universal Primer. The cloning was accomplished following the procedures as described in *Materials and Methods*.

Figure. 1

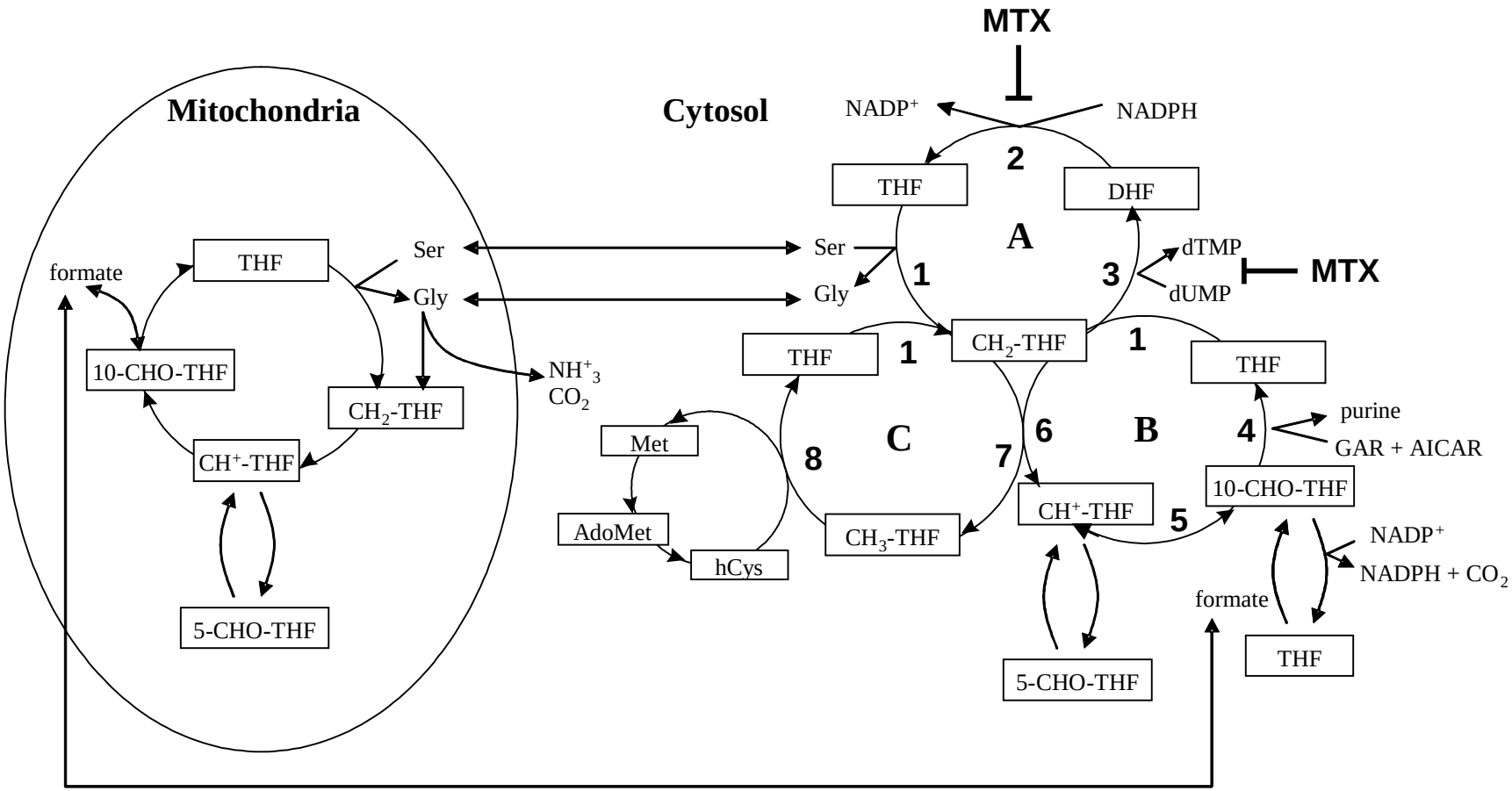

Figure. 2

DMD Fast Forward. Published on July 30, 2007 as DOI: 10.1124/dmd.107.016840
This article has not been copyedited and formatted. The final version may differ from this version.

Figure. 3

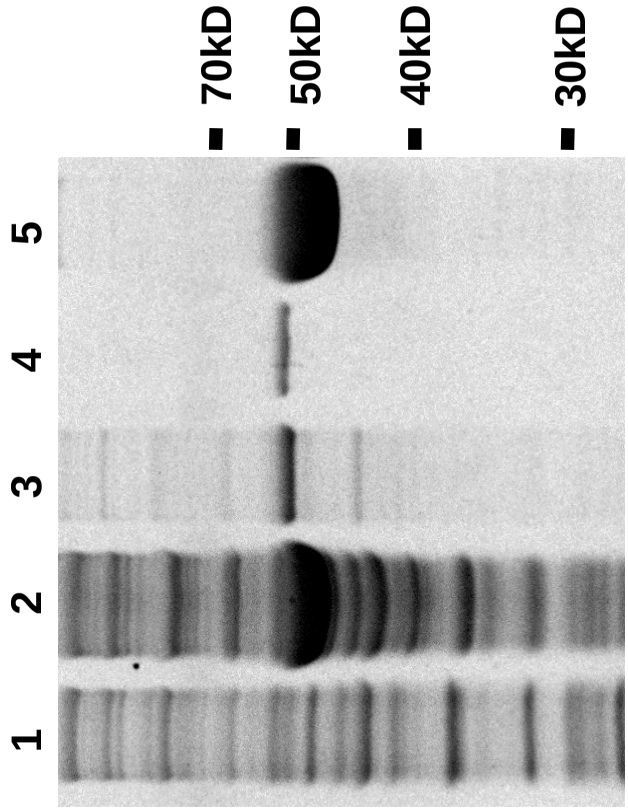

DMD Fast Forward. Published on July 30, 2007 as DOI: 10.1124/dmd.107.016840

Figure. 4

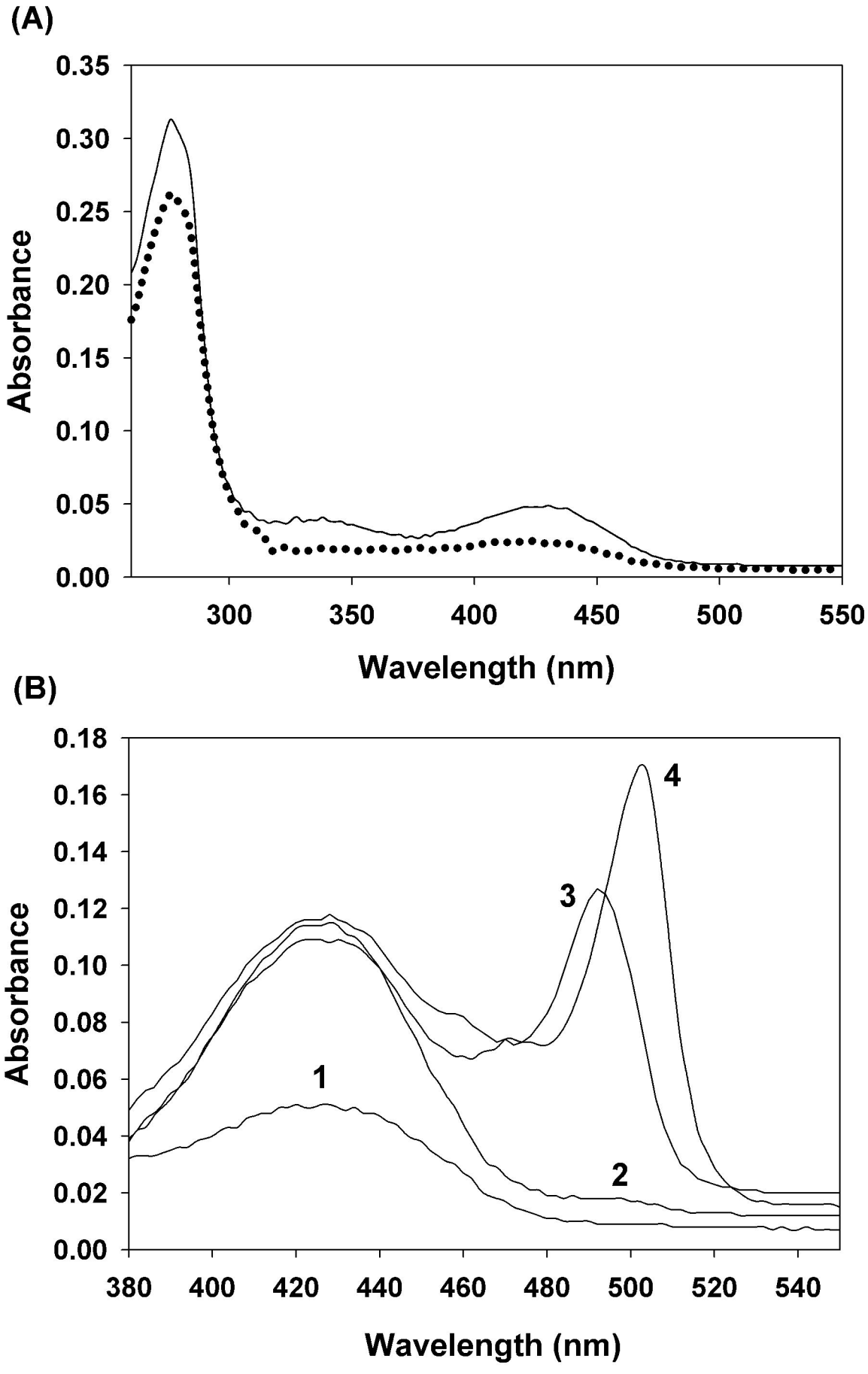

DMD Fast Forward. Published on July 30, 2007 as DOI: 10.1124/dmd.107.016840

Figure. 5

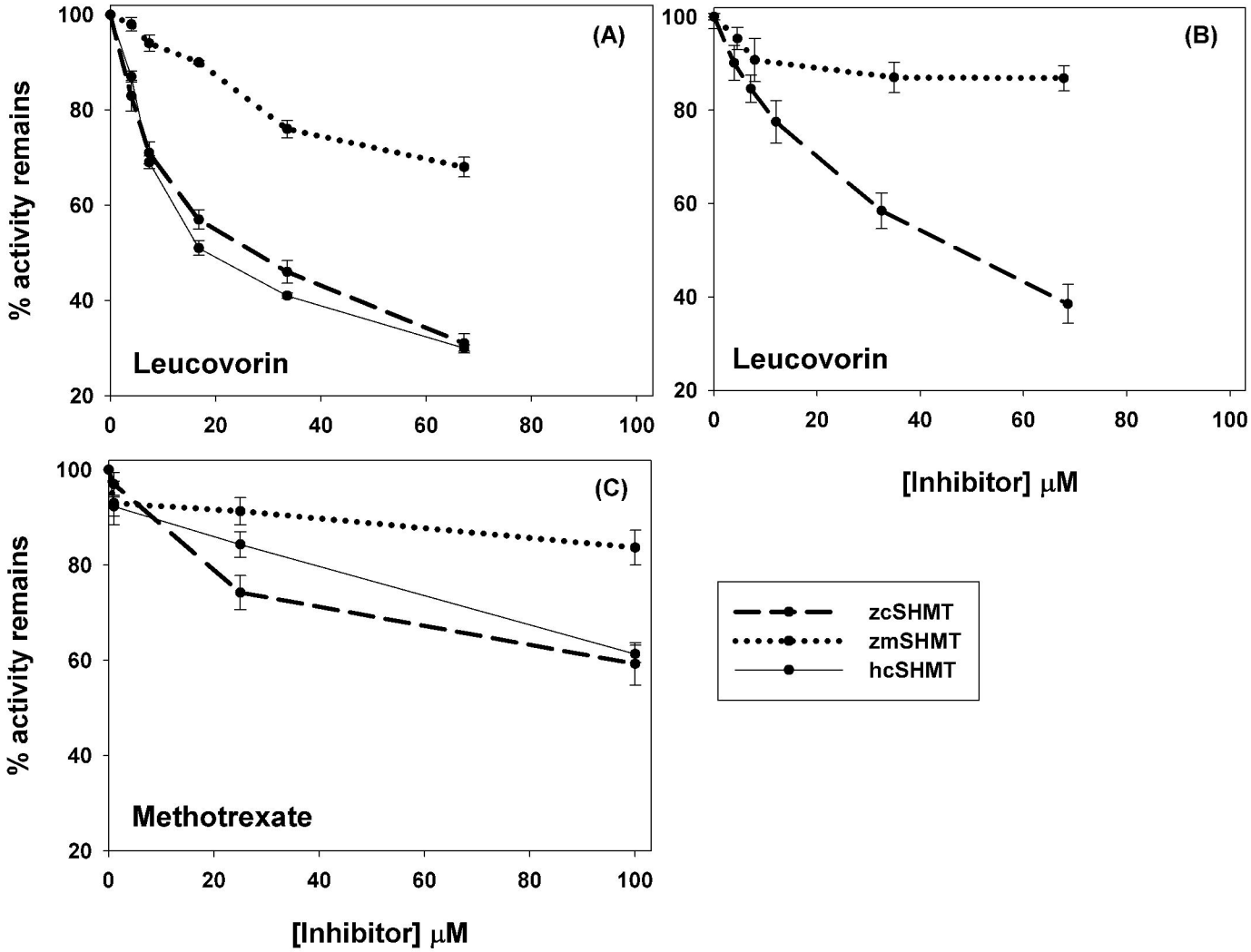

DMD Fast Forward. Published on July 30, 2007 as DOI: 10.1124/dmd.107.016840
This article has not been copyedited and formatted. The final version may differ from this version.

Figure. 6

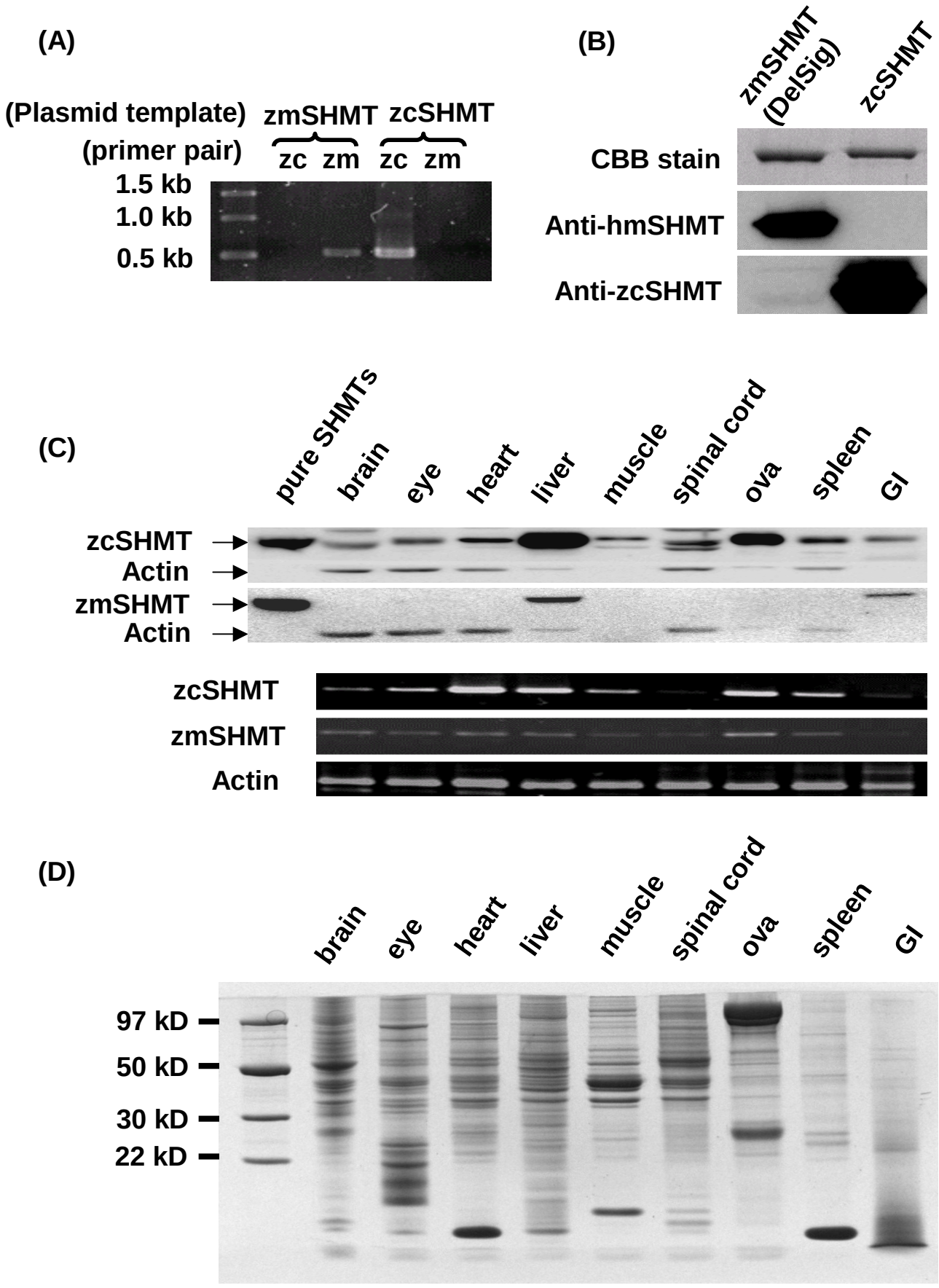

Figure. 7